Proceedings of ASME Turbo Expo 2019
GT2019
June 17-21, 2019, Phoenix, AZ USA

GT2019-90501

Effect of APS flash bond coatings on furnace cycle lifetime of disks and rods

Bruce A. Pint, Michael J. Lance, J. Allen Haynes
Oak Ridge National Laboratory, Materials Science and Technology Division
Oak Ridge, TN 37831-6156 Phone: (865) 576-2897, E-mail: pintba@ornl.gov

Edward J. Gildersleeve and Sanjay Sampath
Center for Thermal Spray Research, Stony Brook University, Stony Brook, NY 11794

ABSTRACT

Air plasma sprayed (APS) flash coatings on high velocity oxygen fuel (HVOF) bond coatings are well known to extend the lifetime of thermal barrier coatings. Recent work compared flash coatings of NiCoCrAlY and NiCoCrAlYHfSi applied to both rods and disk substrates of alloy 247. For rod specimens, 100-h cycles were used at 1100°C in wet air. Both flash coatings significantly improved the lifetime compared to HVOF-only and VPS-only MCrAlY bond coatings with no statistical difference between the two flash coatings. For disk specimens tested in 1-h cycles at 1100°C in wet air, the NiCoCrAlY flash coating significantly outperformed an HVOF-only NiCoCrAlYHfSi bond coating and a NiCoCrAlYHfSi flash coating. The flash coatings formed a mixed oxide-metal zone that appeared to inhibit crack formation and extend lifetime. In addition to the flash coating increasing the bond coating roughness, the underlying HVOF layer acted as a source of Al for this intermixed zone and prevented the oxide from penetrating deeper into the bond coating. The lower Y+Hf level in the Y-only flash coating appeared to minimize oxidation in the flash layer, thereby increasing the benefit compared to a NiCoCrAlYHfSi flash coating.

INTRODUCTION

Fossil fuels continue to represent the majority of electricity generation in the U.S. (>60%) but natural gas has surpassed coal in recent years [1]. It appears that natural gas-fired combined cycle (NGCC) plants will dominate the market for the forseeable future. Increased turbine efficiency can help lower both emissions and the cost of electricity. The pathway to higher efficiency is primarily through increasing the turbine inlet temperature. However, achieving higher temperatures must be accomplished while maintaining the reliability and durability (>25 kh between major overhauls) required by the utility industry. Thus, improved materials solutions are essential to improving efficiency. Considerable effort is focused on ceramic composite hot section components, particularly for aircraft engines [2]. However, Si-based composites must deal with the environmental durability issues caused by water vapor in combustion environments [3]. Also, considerable development is needed to address cost concerns and the larger components needed for land-based turbines. For the near term, current turbines rely on Ni-base superalloys, which are able to reliably operate at very high turbine inlet temperatures (≥1400°C) due to film cooling and thermal barrier coatings (TBC) [4-13].

New TBC concepts are typically first evaluated in furnace cycle testing (FCT) with thermal gradient testing, such as burner rigs, being used for promising TBC concepts before engine testing. Over time, the TBC research effort at Oak Ridge National Laboratory has developed several core focus areas and concepts: (1) large industrial gas turbines use thermally-sprayed coatings [6,9,10], (2) lower cost, polycrystalline superalloys are of interest and have similar TBC lifetimes as single crystal superalloy substrates [14], (3) FCT testing should be conducted in air with water vapor to better simulate turbine exhaust and the negative effects of H_2O on TBC performance [13-24], and (4) in addition to 1-h FCT, 100-h cycles can simulate base-load performance, which might be relevant for integrated gasification combined cycle (IGCC) operation. Recently, the project began incorporating multi-layer top coating architectures [25] and rod specimens [26] as steps towards coating bars for thermal gradient testing. The rod specimens had surprisingly shorter FCT lifetimes compared to those of flat disk specimens [24,27,28]. Based on input from

industry, multi-layer bond coatings with the incorporation of an APS "flash" layer [26] above an HVOF coating layer were evaluated. Preliminary results with multi-layer bond coatings were presented previously [28]. The hypothesis was that flash coatings were effective because of their higher roughness [26]. If that is correct, then perhaps the use of MCrAlYHfSi bond coatings [5,29,30] is not necessary, since their increased FCT lifetime performance, compared to Y-only bond coatings [31] was attributed to the co-doping effect of Y and Hf [32,33] which improves alumina scale adhesion. To address these observations, the current study compares Y-only to MCrAlYHfSi flash coatings on both rod and disk specimens.

EXPERIMENTAL PROCEDURE

Substrates for coating included disk (2mm thick, ~16mm diameter with chamfered edges) and rod specimens (12.5 mm diameter, ~30 mm length) machined from superalloy 247 with composition shown in Table 1. Prior to coating deposition, the specimen surfaces were grit blasted with alumina and then coated using standard commercial-type, air-plasma spray (APS), high velocity oxygen fuel (HVOF) or vacuum plasma spray (VPS) processes. For HVOF and APS, the powder size was 16-88 μm. The two powder compositions are shown in Table 1. The coated substrates were then annealed in a vacuum of 10^{-4} Pa (10^{-6} Torr) for 4h at 1080°C. After annealing, the disks were coated with ~200 μm of standard Y_2O_3-stabilized ZrO_2 (YSZ) deposited by APS. The APS YSZ top coating on the rods was nominally 300 μm thick extra porous YSZ, YSZ with a dense inner layer and extra porous (hi P) outer layer or YSZ with an outer layer of $Gd_2Zr_2O_7$ (YSZ-GDZ) top coating. Thus, the top coating was either a single- or multi-layer structure, as described elsewhere [25]. The various coating combinations evaluated are summarized in Table 2. The surface roughness (R_a) of the bond coatings was measured using a Keyence model VR-3000 optical profilometer or by analysis of light microscopy images.

Average FCT lifetimes of TBC specimens were determined by exposing groups of 3-5 similarly coated rod or disk specimens at each condition. Coating failure was defined as >20% loss of the YSZ layer but, in most cases, the entire top coating spalled in one piece at failure. For 1-h cycle time FCT,

Table 1. Alloy chemical composition (mass %, balance Ni) determined by plasma and combustion analyses.

Alloy	Cr	Al	Co	Ti	Hf	Y	S*	Other
247	8.5	5.7	9.8	1.0	1.4	<	<3	9.9W,3.1Ta,0.7Mo,0.2C
bond coating powders:								
YHfSi	16.7	12.3	21.6	<	.25	.68	2	0.65Si
Y only	16.6	12.8	23.0	<	<	.42	8	0.04Si

* S in ppmw < indicates less than 0.01% or 0.0003% for Y

Table 2. Summary of different coating combinations investigated typically using commercial NiCoCrAlYHfSi (YHS) and YSZ powder except where noted

Substrate	Bond Coating	APS YSZ Top coating
Rod	-HVOF (YHS)	-High porosity (1 layer)
	-HVOF (YHS) + 200μm APS (YHS)	-Bi-layer (inner dense) -Tri-layer (outer $Gd_2Zr_2O_7$)
Rod	-HVOF (YHS) + 50μm APS (YHS) -HVOF (YHS) + 50μm APS (Y only) -VPS (YHS)	-All high porosity (1 layer)
Disk	-HVOF (YHS) -HVOF (YHS) + 50μm APS (YHS) -HVOF (YHS) + 50μm APS (Y only)	-All standard porosity (1 layer)

the specimens were hung by a Pt-Rh wire in an automated cyclic rig and exposed for 1 h at temperature (1100°C) in air with 10±1 vol.% H_2O followed by cooling for 10 min to <30°C in laboratory air for each cycle. For 100-h cycle time FCT, the specimens were placed in an alumina boat, heated to temperature over ~4 h in an alumina tube with flowing argon, held for 100 h in air with 10±1 vol.% H_2O, and then furnace cooled after the cycle in argon. To add water vapor, the carrier gas was typically flowed at 500 ml/min with distilled water atomized into the gas stream above its condensation temperature. The injected water was measured to calibrate its concentration. For weighing, specimens were cooled to room temperature and visually examined. Specimen mass change was measured every 20 cycles or each 100-h cycle using a Mettler-Toledo model XP205 balance.

A Dilor XY800 Raman microprobe (Horiba Scientific, Edison, NJ) with an Innova 308c Ar+ laser (Coherent, Inc., Santa Clara, CA) operating at 5145 Å with a power at the YSZ surface of 10 mW was used to measure residual stresses in the thermally grown alumina scale. Photo-stimulated luminescence piezospectroscopy (PLPS) stress maps were collected on the flat specimens and a line profile was collected along the length of rod specimens. The acquisition time for one spectrum was 0.1-0.5 s and 3,468 and 2001 spectra were collected from the disk and rod specimens, respectively. The location of the map or line was identified by a fiducial marker and the procedure is described elsewhere [14,22,24,27,34]. The laser spot size and the mapping step size were both 10 µm. The intensity of the spectrum measured underneath the YSZ was ~10,000 times weaker compared to a bare bond coating. The stress state was not assumed to be biaxial since the bond coating surface was not flat and the scale cracked, so hydrostatic stress (the average of the trace of the stress tensor) was determined by dividing the frequency shift of the R2 line from a zero stress reference (NIST standard reference material 676A) by 7.61 cm^{-1}/GPa [27]. Due

to the large number of spectra collected, no attempt was made to deconvolute multiple stress states and only a single stress (one set of R-lines) was fitted to each spectrum.

For cross-sectional analyses, the specimens were mounted in epoxy and then cut for metallographical polishing and examination by light microscopy. Additional characterization of the disk specimens is presented elsewhere [35].

RESULTS

Rod specimens

Figure 1 shows the final FCT results from the previous study where the rods with an HVOF-only MCrAlYHfSi bond coating showed very low lifetimes in 100-h cycles at 1100°C [28]. The addition of an APS MCrAlYHfSi layer over the HVOF layer greatly increased the FCT lifetime under these conditions. The different top coatings did not appear to affect the behavior. Figure 2 shows examples of failed specimens. Figure 2a shows one of the bi-layer top coatings after spallation of the top coating after 26, 100-h cycles. A thick alumina layer formed at the bond coating-top coating interface. This layer is shown at higher magnification in Figure 2b for a high porosity YSZ specimen cycled for 36, 100-h cycles before failure. Compared to the as-deposited coating [28], the internal oxidation (dark areas) in the APS layer, particularly near the HVOF interface, has significantly increased with exposure.

Figure 3 compares the residual stress in an HVOF-only disk and APS-coated rod specimens exposed in 100-h cycles. While maps can be produced for the flat specimens and measured at the same location over time [14,22,24,27,34], this is not

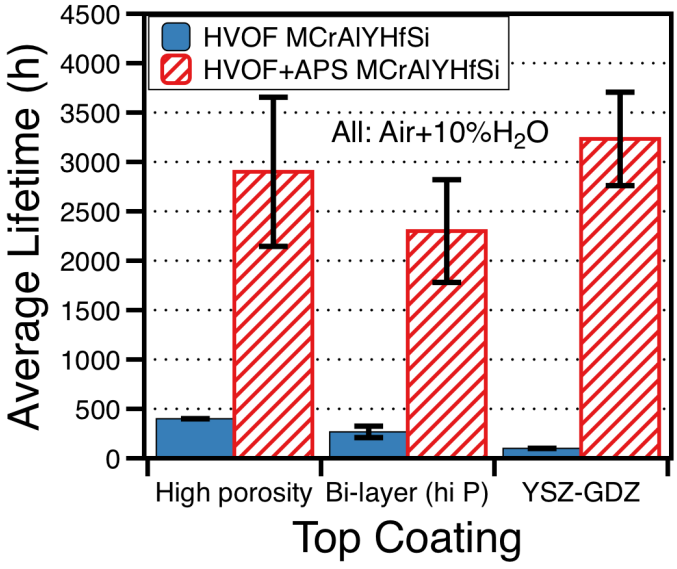

Figure 1. Average coating lifetimes (cumulative time in 100-h cycles to failure) for rod specimens with two bond coatings and three different top coatings. Whiskers note a standard deviation for 3 specimens of each type.

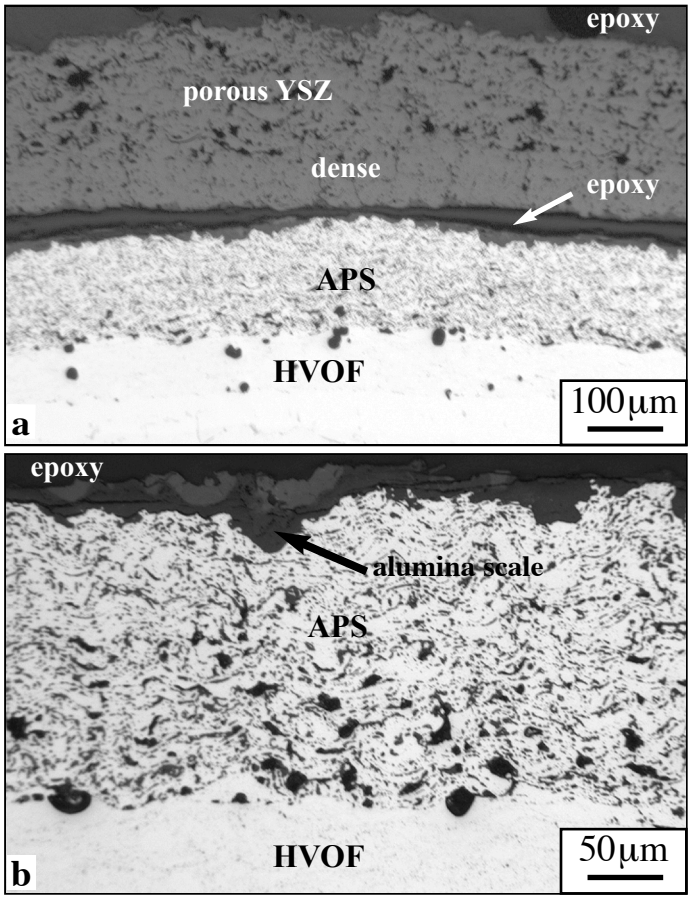

Figure 2. Light microscopy of polished cross-sections of failed APS+HVOF bond coatings on 247 rods after 100-h cycles at 1100°C in wet air (a) bi-layer YSZ, 26 x 100h and (b) high porosity YSZ, 36 x 100h cycles.

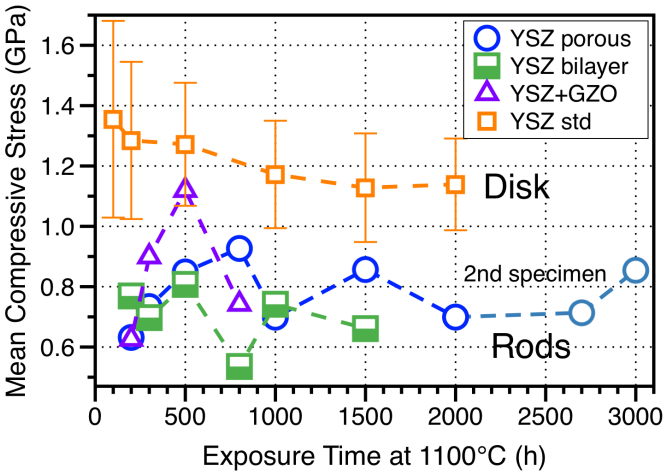

Figure 3. Residual compressive stress in the alumina scale measured by PSLS on 247 disk and rod specimens as a function of exposure time in 100-h cycles at 1100°C. Additional measurements were made on a second high porosity specimen after the first specimen failed.

possible for the rods and only an average compressive stress value is obtained for the rod specimen line profiles. The measurement was further complicated by the 300 μm top coating thickness on the rod specimens. In some cases, the measurements were stopped because no signal could be obtained through the YSZ at longer exposure times. For comparison, a similar value was averaged for the disk specimen. Interestingly, the residual stresses were consistently higher on the disk specimen, perhaps because of the flatter interface compared to the APS-coated rod specimens. Recall from Figure 1 that the lifetimes were very short for the HVOF-only rod specimens so no similar long-term comparison could be made between disks and rods with the same bond coating. Perhaps the lower residual stresses for rod specimens is an indication of more damage to the alumina scale because of the interface geometry.

While the results in Figure 1 showed a large increase in FCT lifetimes when the APS layer was added, the thick APS layer was not like the ~50 μm APS "flash" coating described previously [26] and there was concern that the lifetime increase was due to the thicker bond coating. Therefore, another batch of specimens was made with a thinner APS layer. Also, the hypothesis was that the flash coating was effective because of its high roughness [26]. That led to two questions: (1) VPS coatings can have high roughness, how do they compare on rod specimens? and (2) if roughness is key, are MCrAlYHfSi coating compositions needed? Figure 4 shows the results of the next phase of FCT testing of rods in 100-h cycles at 1100°C. For comparison, the average lifetime for HVOF-only disks is also shown. Figure 5 shows the as-deposited VPS coating on a 247 rod with an interface roughness of ~9 μm (R_a). However, the lifetime did not match the excellent lifetime observed for the 50 μm thick APS flash coatings, Figure 4. For the two types of flash coatings, with and without Hf+Si additions, the large variation in lifetimes (large standard deviations) makes their behavior statistically similar. One Y-only flash coated specimen failed after 54 cycles. Figure 6 shows the flash-coated bond coating after similar failure times. Very thick alumina formed within the outer bond coating layer in both cases. This mixed metal-alumina layer may have inhibited crack propagation at the interface resulting in a long average FCT lifetime. In both cases, the underlying HVOF layer prevented the internal oxidation from penetrating further and affecting the underlying alloy 247 substrate.

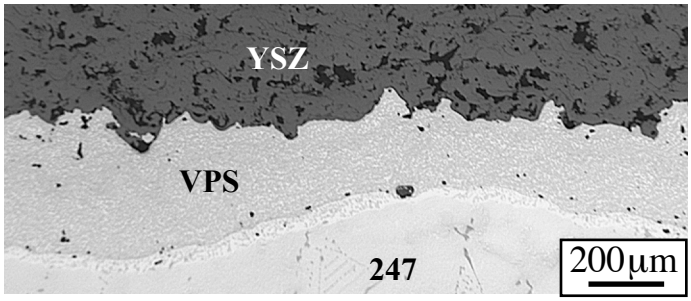

Figure 5. Light microscopy of polished cross-section of as-coated VPS MCrAlYHfSi bond coating on 247 rod with high porosity YSZ.

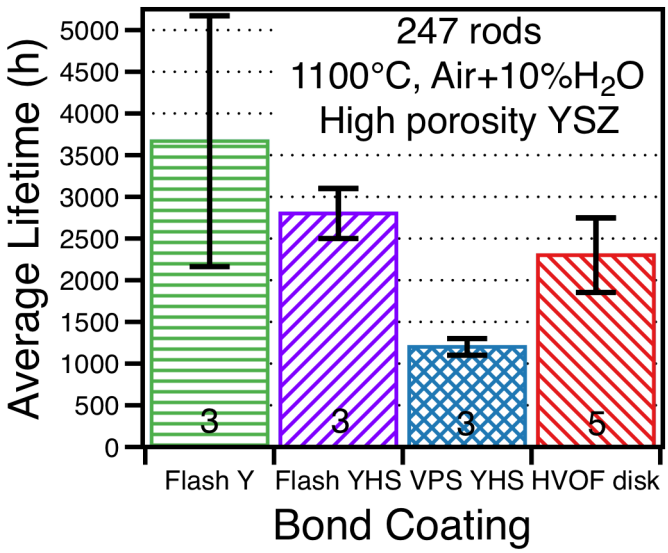

Figure 4. Average lifetime for the next phase of alloy 247 rod specimens with high porosity YSZ top coatings combinations on alloy 247 substrates exposed in 100-h cycles at 1100 °C in air+10%H_2O. Results for disk specimens are shown for comparison. Whiskers note a standard deviation for 3-5 specimens of each type.

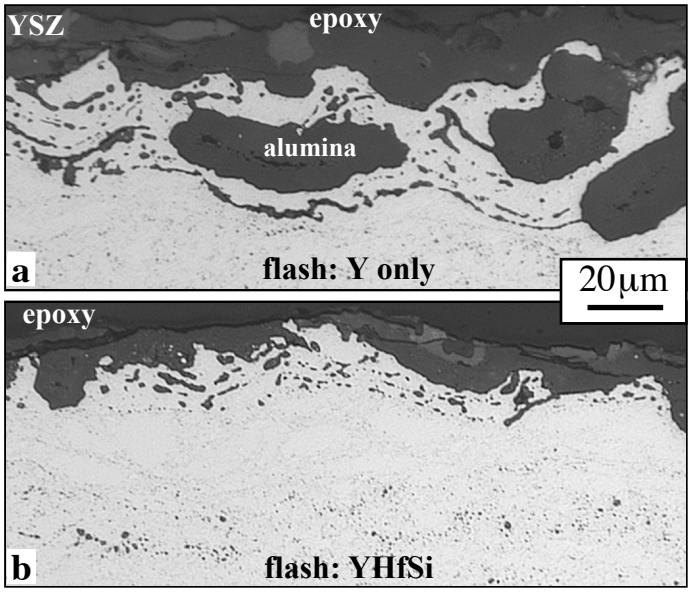

Figure 6. Light microscopy of polished cross-sections of failed APS flash bond coatings on 247 rods after 100-h cycles at 1100°C in wet air (a) Y-only APS bond coating after 29, 100-h cycles and (b) MCrAlYHfSi APS bond coating after 28, 100-h cycles.

Disk specimens

The effectiveness of the APS flash coatings for the rod specimens raised a question about how a flash coating would perform on disk specimens. Thus, a similar experiment was conducted using 1-h cycles. Figure 7 shows the starting flash coatings. It appeared that more oxide formed during deposition of the APS MCrAlYHfSi layer compared to the MCrAlY layer. In addition, a batch of HVOF-only disk specimens were prepared and all of the three types of bond coatings received the same standard porosity YSZ layer, Table 2. Figure 8 shows the measured roughness values for the three bond coatings. In addition to the R_a values, the fractal dimension roughness was calculated similar to the method previously reported [26]. The flash coatings did slightly increase the roughness compared to the HVOF-only roughness values.

The FCT results are shown in Figure 9. Each batch contained 5 specimens of each coating type. The HVOF-only results were compared to a second batch of 3 coatings reported previously and exposed in 2015 [36]. Unlike previous 1-h FCT experiments where the results were not statistically significant [24,34], these results showed significant improvements for the flash coatings compared to the HVOF-only lifetimes and the Y-only flash coatings showed a >70% increase in the average FCT lifetime.

Figure 10 shows representative cross-sections of failed specimens of each type of bond coating. The failed HVOF-only

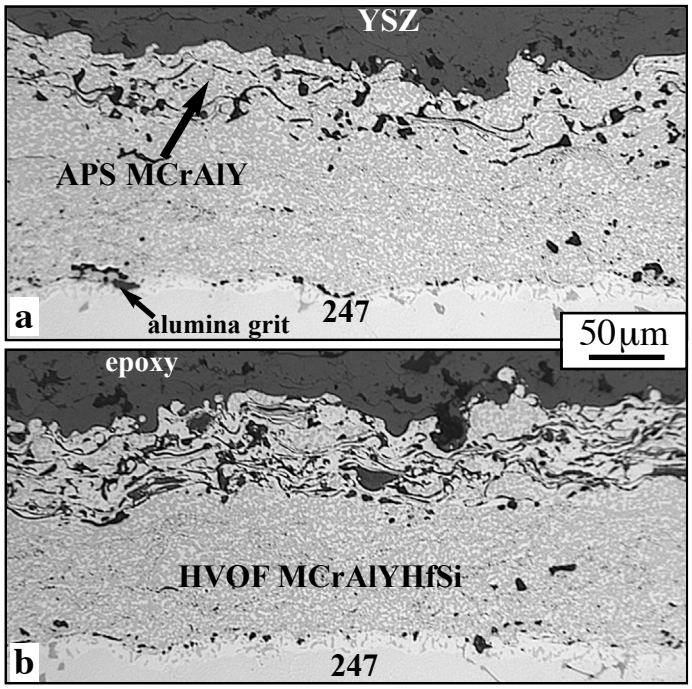

Figure 7. Light microscopy of polished cross-sections of as-coated 247 disks with an inner HVOF MCrAlYHfSi layer and an outer APS flash coating with (a) Y only and (b) YHfSi.

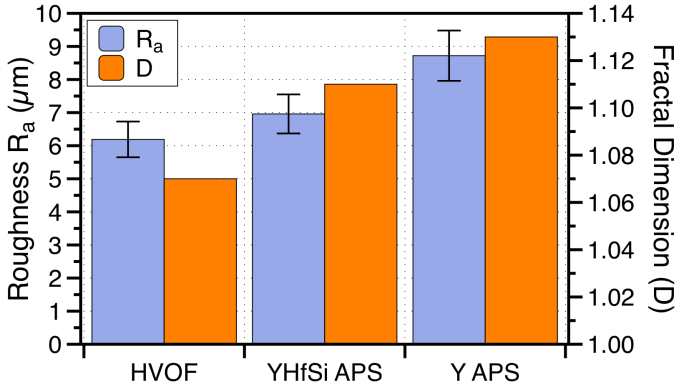

Figure 8. Measured coating roughness on disk specimens

coating appears similar to prior studies [22,31] with a fairly uniform alumina scale formed at the bond coating-top coating interface and minimal internal oxidation, Figure 10a. The flash coated specimens show a highly oxidized morphology with the APS layer significantly consumed and thick oxide formed. Despite only being exposed for 680 cycles, the APS MCrAlYHfSi layer appeared to be more heavily oxidized than the Y-only layer, Figures 10b and 10c, respectively. In both cases, the HVOF layer appeared intact with no significant attack of the 247 substrate.

Because of the difference in exposure time in Figure 10, a more uniform comparison was obtained by taking a 6th specimen of each flash coated specimen and exposing it for various cycle intervals and removing a piece for characterization at 0 cycles (Figure 7) and 100 cycles (Figure

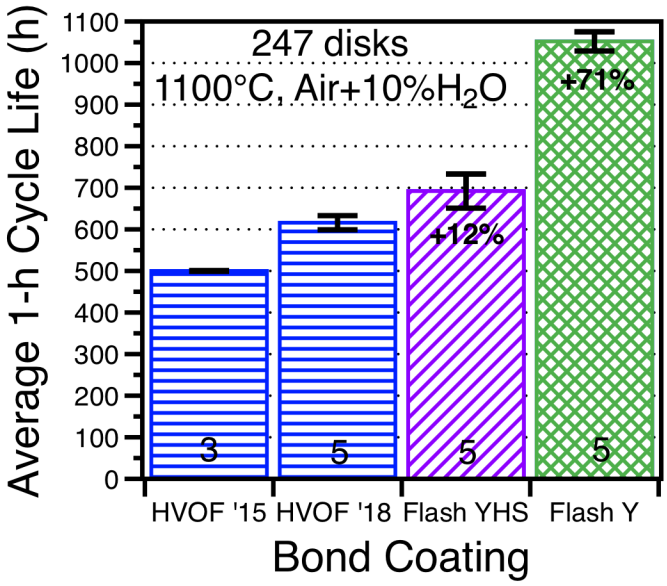

Figure 9. Comparison of average coating lifetimes (cumulative time in 1-h cycles to failure) for alloy 247 disk specimens with various bond coatings tested at 1100°C in wet air [36].

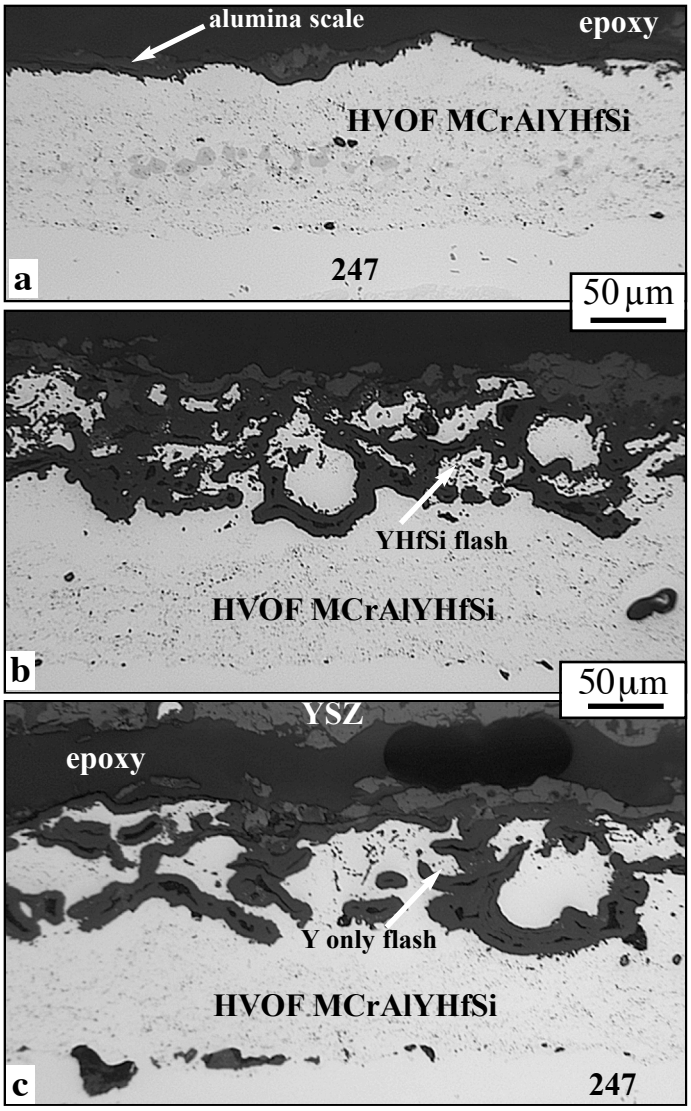

Figure 10. Light microscopy of polished cross-sections of coated 247 disks exposed in 1-h cycles at 1100°C in wet air (a) HVOF MCrAlYHfSi after 620 cycles (b) flash YHfSi bond coating after 680 cycles and (c) flash Y only after 1060 cycles.

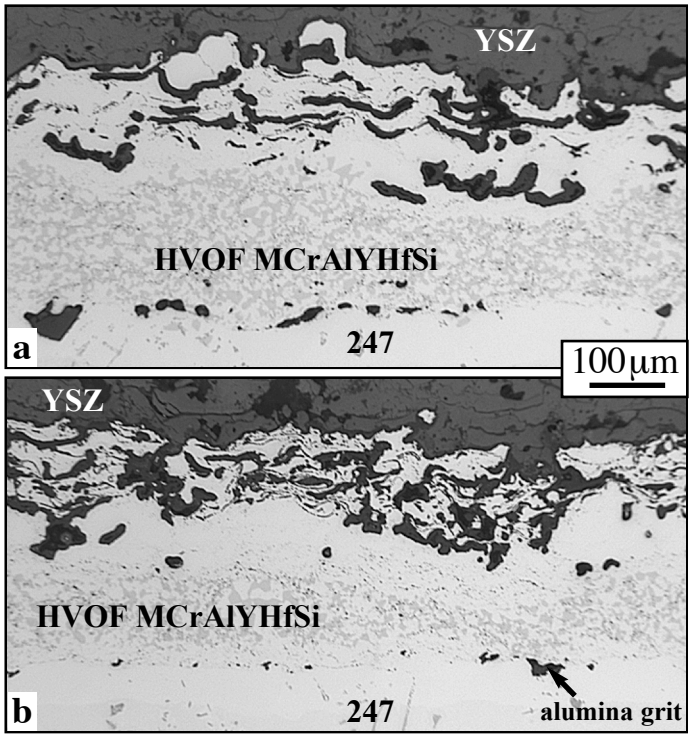

Figure 11. Light microscopy of polished cross-sections of flash coated 247 disks after 100, 1-h cycles at 1100°C in air+10%H_2O (a) Y-only flash coating and (b) YHfSi flash coating.

11). Results after 300 cycles are reported elsewhere [35]. After 100 cycles, there appears to be a clear difference between the two flash coatings with significantly more oxide formed with the YHfSi coating, which contained significantly more Y+Hf than the Y-only coating, Table 1. It appears that for these thin APS layers, the Y-only powder produces a better FCT lifetime because oxidation is minimized in this outer layer.

DISCUSSION

The FCT results for both disks and rods confirms the benefit of an APS flash coating previously reported [26]. Increased roughness could explain the benefit, however, for the rod specimens, VPS bond coatings also show a high roughness but only provided a 3X increase in average FCT lifetime (12 cycles) compared to HVOF-only bond coatings (4 cycles), Figures 1 and 4. In contrast, the flash coatings increased the lifetime by 7-8X. For the disk specimens, the increase in roughness, measured by Ra or fractal dimension (Figure 8), did not appear to predict the large increase in lifetime for the Y-only flash coating, Figure 9. Certainly high roughness is needed for thermally sprayed coatings, but increased roughness may not capture the entire benefit.

Considering the failed sections in Figure 10, the flash coating benefit also might be related to the mixed metal-alumina layer formed at the interface between the HVOF layer and the YSZ top coating. This layer may be extremely difficult for an interfacial crack to propagate through. In the case of an APS-only bond coating, the internal oxidation would include the entire bond coating. However, for this two layer structure, the HVOF layer prevents the oxidation from reaching the substrate. The thicker APS layer in Figure 2b illustrates how internal oxidation permeates the entire coating from top to bottom. One problem with forming a mixed metal-oxide layer in an oxidizing environment is the increased metal-oxide surface area, Figures 10b and 10c, increases the rate of Al consumption. Another benefit of the underlying HVOF layer is that it can act as an Al reservoir for the metal in the mixed layer, supplying fast-

diffusing Al to the reaction front to maintain the mixed structure.

An analysis of Figures 7, 10 and 11 suggests that using MCrAlYHfSi powder to make the APS layer results in much more oxide formation and thus a faster Al consumption rate, which leads to a shorter lifetime. The Y-only flash layer appeared to have coarser metal particles remaining in Figure 10c, however, both coatings were deposited with the same powder size. The increased oxidation with Y and Hf resulted in more oxide formation in the as-deposited coating and after only 100 cycles, Figures 7 and 11. The smaller Y content in the MCrAlY flash coating appears to be an advantage and suggests the powder composition of the APS flash layer might be further optimized. A similar large increase in FCT lifetime was not observed for the Y-only flash coating on rod specimens tested in 100-h cycles. This may have been due to the small (3) number of specimens tested in this experiment. The average was higher for the Y-only specimens but it was not statistically significant as suggested by the high standard deviations.

The majority of FCT testing is conducted on flat specimens. One reason for moving to rod specimens is to eliminate edge failures. Also, turbine components are not flat. The change in geometry to rod specimens resulted in unexpected complications including the 5-6X decrease in FCT lifetime with HVOF-only bond coatings (compare rods in Figure 1 with disks in Figure 4). It is not clear why this decrease in lifetime occurred but the rapid propagation of the interfacial crack suggests that a round geometry magnifies the importance of roughness in preventing crack propagation. However, switching to the rougher VPS bond coating did not fully recover the 5-6X decrease in lifetime, Figure 4. The mixed metal-oxide layer created with the flash coating appears ideal for rod specimens. The residual stress data in Figure 3 suggests that more alumina scale cracking occurs on rod specimens. However, this may also be a product of the higher roughness with the flash coating and the highly non-planar alumina reaction product formed, Figure 2. Residual stress is highest for a flat alumina scale where the compressive cooling stress remains in the plane parallel to the interface. A more sophisticated analysis of the failure mechanism on these various specimens may be needed to fully understand these results.

The improvement in rod FCT lifetime is an important step in testing multi-layer top coatings. Without a thermal gradient, there is no benefit of switching to a lower thermal conductivity GDZ top coating. This work has identified the need to optimize coating deposition parameters based on substrate geometry. Also, both the flash bond coating and the higher porosity YSZ top coating are parameters that need to be investigated in burner rig testing.

CONCLUSION

The addition of an APS flash coating on a dense HVOF bond coating were shown to increase average lifetime in FCT of both rod and flat disk specimens. Flash coatings were fabricated using similar NiCoCrAlY and NiCoCrAlYHfSi powders. For rod specimens, both coatings were more effective than HVOF-only or VPS-only bond coatings using 100-h cycles at 1100°C in wet air. For disk specimens tested using 1-h cycles, the ~50 μm Y-only flash coating increased the FCT lifetime by >70%, while the MCrAlYHfSi flash coating resulted in only a 12% increase compared to an HVOF-only bond coating. The flash coatings formed a mixed oxide-metal zone between the HVOF inner layer and the YSZ top coating that appeared to inhibit crack formation and extend lifetime. In addition to the flash coating increasing the bond coating roughness, the underlying HVOF layer acted as a source of Al for this intermixed zone and prevented the oxide from penetrating deeper into the bond coating. The lower Y+Hf level in the Y-only flash coating appeared to minimize oxidation in the flash layer, thereby increasing the benefit compared to a NiCoCrAlYHfSi flash coating.

ACKNOWLEDGMENTS

The authors would like to thank G. W. Garner, T. M. Lowe, M. Stephens and T. Jordan at ORNL for assistance with the experimental work and A. Hague of Mitsubishi Hitachi Power Systems for the VPS coatings. S. Dryepondt and E. Lara-Curzio provided helpful comments on the manuscript. This research was sponsored by the U.S. Department of Energy, Office of Fossil Energy, Turbine Program (R. Dennis program manager). This manuscript has been authored by UT-Battelle, LLC under Contract No. DE-AC05-00OR22725 with the U.S. Department of Energy. The United States Government retains and the publisher, by accepting the article for publication, acknowledges that the United States Government retains a non-exclusive, paid-up, irrevocable, world-wide license to publish or reproduce the published form of this manuscript, or allow others to do so, for United States Government purposes. The Department of Energy will provide public access to these results of federally sponsored research in accordance with the DOE Public Access Plan (http://energy.gov/downloads/doe-public-access-plan).

REFERENCES

1. https://www.eia.gov/energyexplained, accessed Nov. 2018.
2. Naslain, R., 2004, “Design, preparation and properties of non-oxide CMCs for application in engines and nuclear reactors: an overview,” Composites Sci. Technol., **64**, No.2, pp.155-170.
3. Eaton, H. E. and Linsey, G. D., 2002, “Accelerated oxidation of SiC CMC’s by water vapor and protection via environmental barrier coating approach,” Journal of the European Ceramic Society **22**, pp.2741–2747
4. Bennett, A., 1986, "Properties of Thermal Barrier Coatings," Materials Science and Technology, **2**, pp.257-

261.
5. DeMasi-Marcin, J. T. and Gupta, D. K., 1994, "Protective coatings in the gas turbine engine," Surface and Coatings Technology, **68-69**, pp.1–9.
6. Nelson, W. A. and Orenstein, R. M., 1997, "TBC Experience in Land-Based Gas Turbines," Journal of Thermal Spray Technology, **6,** No.2, pp.176-180.
7. Goward, G. W., 1998, "Progress in Coatings for Gas Turbine Airfoils," Surface and Coatings Technology, **108-109**, pp.73-79.
8. Pint, B. A., Wright, I. G., Lee, W. Y., Zhang, Y., Prüßner, K. and Alexander, K. B., 1998, "Substrate and Bond Coat Compositions: Factors Affecting Alumina Scale Adhesion," Mater. Sci. Eng. A, **245**, pp.201-211.
9. Stringer, J., 1998, "Coatings in the electricity supply industry: past, present, and opportunities for the future," Surface and Coatings Technology, **108–109**, pp.1–9.
10. Itoh, Y., Saitoh, M. and Tamura, M., 2000, "Characteristics of MCrAlY Coatings Sprayed by High Velocity Oxygen-Fuel Spraying System," Journal of Engineering for Gas Turbines and Power, **122**, pp.43-49.
11. Nicholls, J. R., 2003, "Advances in Coating Design for High-Performance Gas Turbines," MRS Bulletin, **28**, pp.659-670.
12. Gleeson, B., 2006, "Thermal Barrier Coatings for Aeroengine Applications," Journal of Propulsion and Power, **2**, pp.375-383.
13. Naumenko, D., Pillai, R., Chyrkin, A., Quadakkers, W. J., 2017, "Overview on Recent Developments of Bondcoats for Plasma-Sprayed Thermal Barrier Coatings," Journal of Thermal Spray Technology **26**, pp.1743-1757.
14. Lance, M. J., Unocic, K. A., Haynes, J .A. and Pint, B. A., 2015, "APS TBC Performance on Directionally-Solidified Superalloy Substrates with HVOF NiCoCrAlYHfSi Bond Coatings," Surface and Coatings Technology, **284**, 9-13.
15. Leyens, C., Fritscher, K., Gehrling, R., Peters, M. and Kaysser, W. A., 1996, "Oxide Scale Formation on an MCrAlY Coating in Various H_2-H_2O Atmospheres," Surface and Coatings Technology, **82**, pp.133-144.
16. Janakiraman, R., Meier, G. H. and Pettit, F. S., 1999, "The Effect of Water Vapor on the Oxidation of Alloys that Developed Alumina Scales for Protection," Metallurgical and Materials Transactions, **30A**, pp.2905-2913.
17. Onal, K., Maris-Sida, M. C., Meier, G. H. and Pettit, F. S., 2003, "Water Vapor Effects on the Cyclic Oxidation Resistance of Alumina-Forming Alloys," Materials at High Temperature, **20**, pp.327-337.
18. Pint, B. A., Haynes, J. A., Zhang, Y., More, K. L. and Wright, I. G., 2006, "The Effect of Water Vapor on the Oxidation Behavior of Ni-Pt-Al Coatings and Alloys," Surface and Coatings Technology, **201**, pp.3852-3856.
19. Smialek, J. L., 2008, "Enigmatic Moisture Effects on Al_2O_3 Scale and TBC Adhesion," Materials Science Forum, **595-598**, pp.191-198.
20. Déneux, V., Cadoret, Y., Hervier, S. and Monceau, D., 2010, "Effect of Water Vapor on the Spallation of Thermal Barrier Coating Systems During Laboratory Cyclic Oxidation Testing," Oxidation of Metals, **73**, pp.83-93.
21. Pint, B. A., Garner, G. W., Lowe, T. M., Haynes, J. A. and Zhang, Y., 2011, "Effect of increased water vapor levels on TBC lifetime with Pt-containing bond coatings," Surface and Coatings Technology, **206**, pp.1566-1570.
22. Lance, M. J., Unocic, K. A., Haynes, J. A. and Pint, B. A., 2014, "The Effect of Cycle Frequency, H_2O and CO_2 on TBC Lifetime with NiCoCrAlYHfSi Bond Coatings," Surface and Coatings Technology, **260**, pp.107-112.
23. Pint, B. A., Unocic, K. A. and Haynes, J. A., 2016, "The Effect of Environment on TBC Lifetime," Journal of Engineering for Gas Turbines & Power, **138**, No.8, 082102.
24. Pint, B. A., Haynes, J. A., Lance, M. J., Aldridge, Jr., H. L., Viswanathan, V., Dwivedi, G. and Sampath, S., 2016, "Factors Affecting TBC Furnace Cycle Lifetime: Temperature, Environment, Structure and Composition," in M. Hardy, et al. eds., Superalloys 2016, TMS, Warrendale, PA, pp.727-734.
25. Viswanathan, V., Dwivedi, G. and Sampath, S., 2014, "Engineered Multilayer Thermal Barrier Coatings for Enhanced Durability and Functional Performance," Journal of the American Ceramic Society **97**, pp.2770-2778.
26. Nowak, W., Naumenko, D., Mor, G., Mor, F., Macka, D. E., Vassena, R., Singheiser, L. and Quadakkers, W. J., 2014, "Effect of processing parameters on MCrAlY bondcoat roughness and lifetime of APS–TBC systems," Surface and Coatings Technology, **260**, pp.82–89.
27. Lance, M. J., Haynes, J .A., Pint, B. A., 2016, "The Effects of Temperature and Substrate Curvature on TBC Lifetime and Residual Stress in Alumina Scales beneath APS TBCs," Surface and Coatings Technology, **308**, pp.19-23.
28. Pint, B. A., Lance, M. J., Haynes, J. A., (2019) "The Effect of Coating Composition and Geometry on TBC Lifetime," Journal of Engineering for Gas Turbines and Power **141**, no.031004.
29. Gupta, D. K. and Duvall, D. S., 1984, "A Silicon and Hafnium Modified Plasma Sprayed MCrAlY Coating for Single Crystal Superalloys," Superalloys 1984, ed. M. Gell, et al. (Warrendale, PA: TMS), 711-720.
30. Unocic, K. A. and Pint, B. A., 2010, "Characterization of the Alumina Scale Formed on a Commercial MCrAlYHfSi Coating," Surface and Coatings Technology, **205**, pp.1178-1182.
31. Haynes, J. A., Unocic, K. A. and Pint, B. A., 2013, "Effect of Water Vapor on the 1100°C Oxidation Behavior of Plasma-Sprayed TBCs with HVOF NiCoCrAlX Bond Coats," Surface and Coatings Technology, **215**, pp.39-45.
32. Pint, B. A., More, K. L., Wright, I. G., 2003, "The Use of Two Reactive Elements to Optimize Oxidation Performance of Alumina-Forming Alloys" Materials at High Temperature **20**, 375-86.

33. Unocic, K. A. and Pint, B. A., 2013, “Oxidation Behavior of Co-Doped NiCrAl Alloys in Dry and Wet Air,” Surface and Coatings Technology, **237**, pp.8-15.
34. Lance, M. J., Unocic, K. A., Haynes, J. A. and Pint, B. A., 2013, “Effect of Water Vapor on Thermally Grown Alumina Scales on Simple and Pt-modified Aluminide Coatings,” Surface and Coatings Technology, **237**, pp.2-7.
35. Lance, M. J., Thiesing, B. P., Haynes, J. A., Parish, C. M. and Pint, B. A., 2018, “The Effect of HVOF Bond Coating with APS Flash Coating on TBC Performance,” Oxidation of Metals, submitted.
36. Lance, M. J., Haynes, J. A. and Pint, B. A., 2018, “Performance of Vacuum Plasma Spray Bond Coatings at 900° and 1100°C,” Surface & Coatings Technology **337**, pp.136–140.